Modeling solar dynamics

Manfred Küker

Leibniz-Institut für Astrophysik Potsdam

Flux transport dynamo

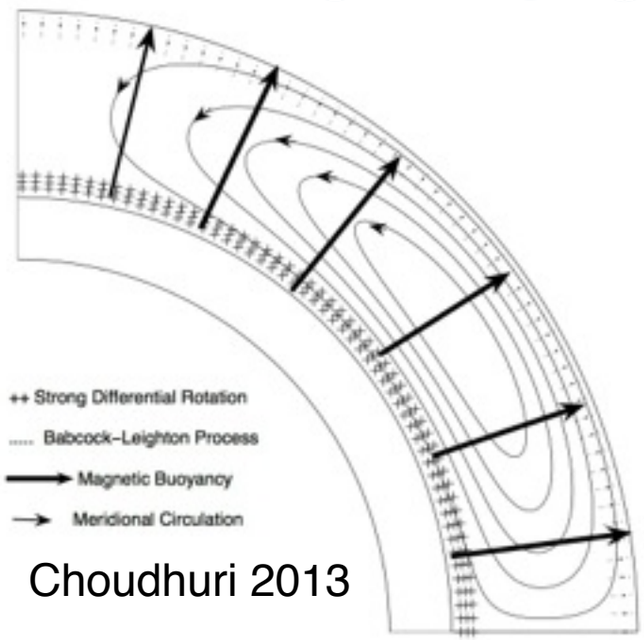

Choudhuri 2013

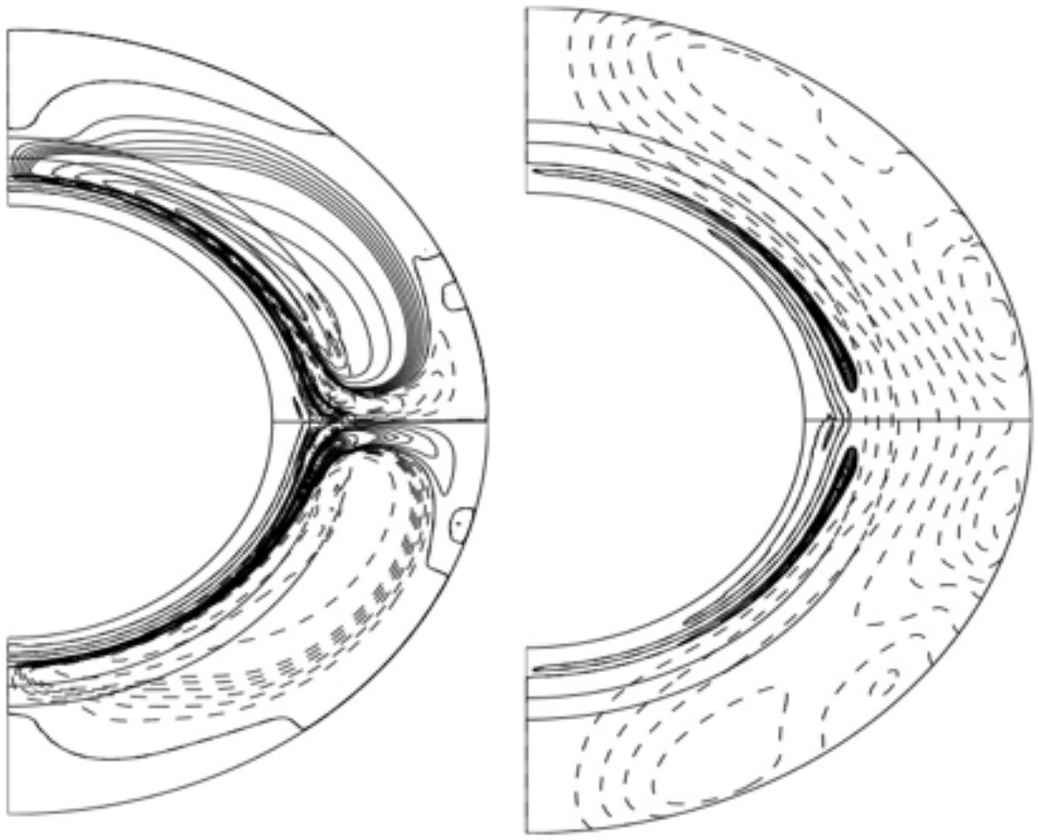

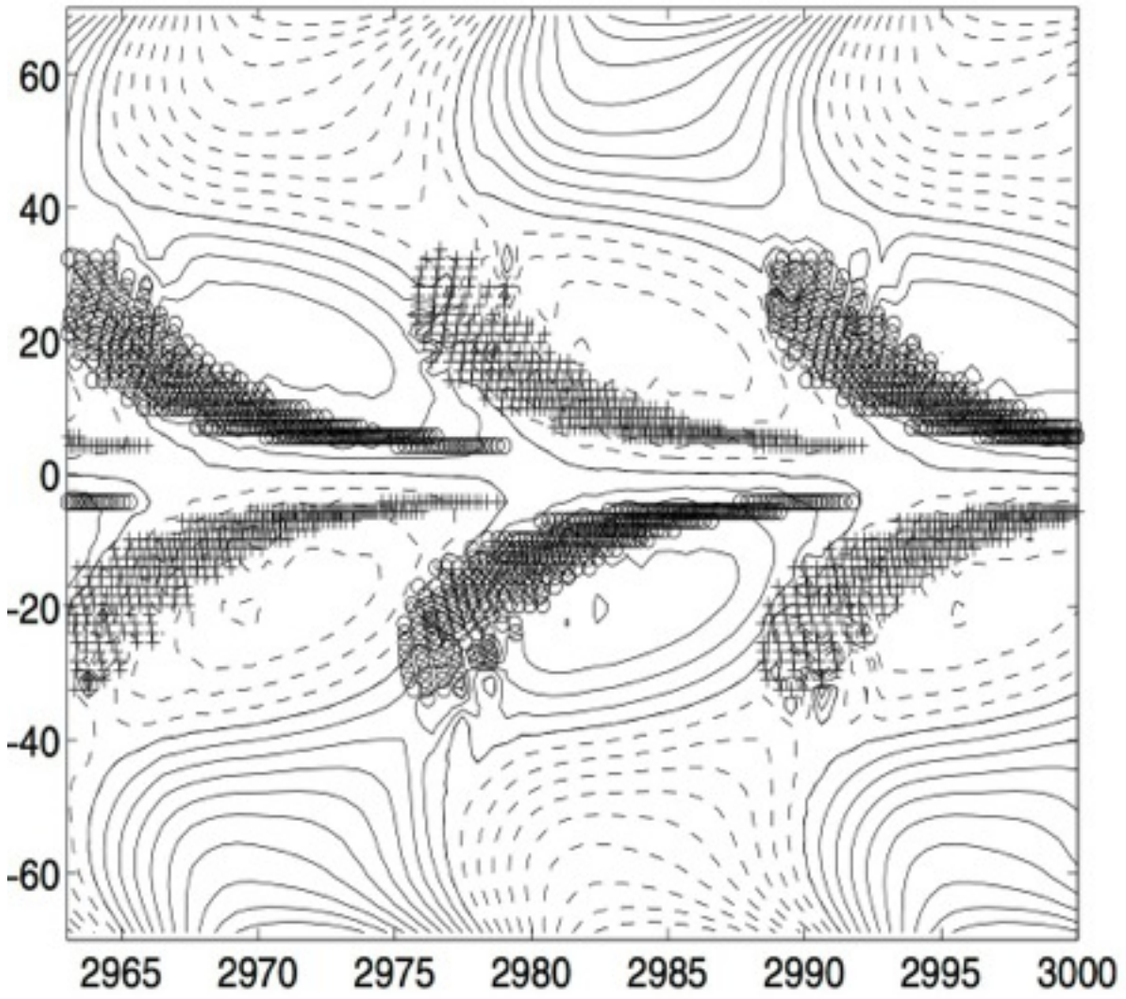

Chatterjee et al. 2004

Flux transport dynamo: problems

- model assumptions not well constrained
- requires peculiar choice of magnetic diffusion coeff. for parity selection
- merid. flow penetrates into tachocline
- strictly kinematic

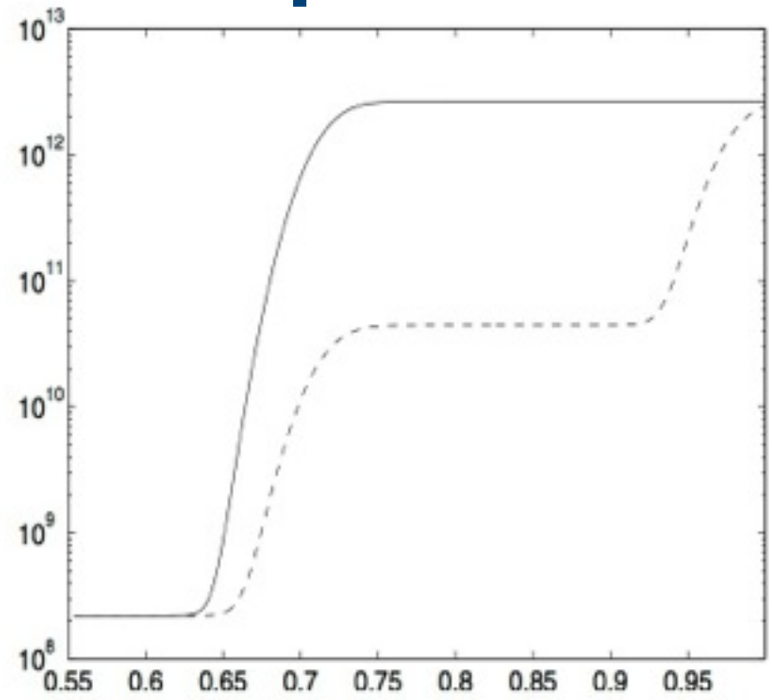

Fig. 4. Plots of $\eta_p(r)$(solid) and $\eta_t(r)$ (dashed) as given by Eqs. (12) and (13) as functions of the fractional radial distance $(r/R_\odot)$. The y-axis is in units of $cm^2\ s^{-1}$

Chatterjee et al. 2004

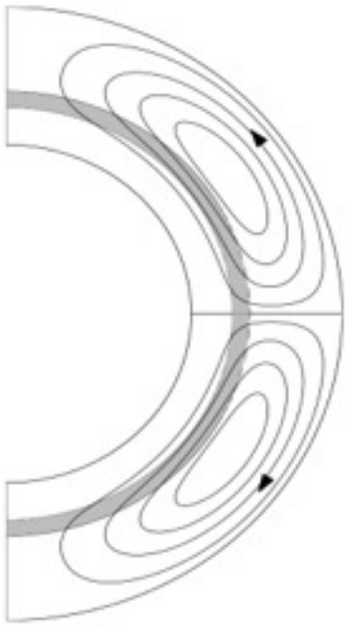

Mean field MHD

Mean field ansatz:

$$\boldsymbol{u} = \bar{\boldsymbol{u}} + \boldsymbol{u}' \qquad \boldsymbol{B} = \bar{\boldsymbol{B}} + \boldsymbol{B}'$$

Reynolds equation:

$$\rho \left[\frac{\partial \bar{\boldsymbol{u}}}{\partial t} + (\bar{\boldsymbol{u}} \cdot \nabla) \bar{\boldsymbol{u}} \right] = -\nabla \cdot \rho Q - \nabla P + \rho \boldsymbol{g}$$

Heat transport:

$$\rho T \frac{\partial \bar{s}}{\partial t} + \rho T \bar{\boldsymbol{u}} \cdot \nabla \bar{s} = -\nabla \cdot \left(F^{\mathrm{conv}} + F^{\mathrm{rad}} \right) + \epsilon$$

Induction equation:

$$\frac{\partial \bar{\boldsymbol{B}}}{\partial t} = \nabla \times (\bar{\boldsymbol{u}} \times \bar{\boldsymbol{B}} - \eta \nabla \times \bar{\boldsymbol{B}} + \mathcal{E})$$

Transport coefficients

Correlation tensor: $$Q_{ij} = \overline{u_i' u_j'}$$

Rotating frame: $$Q_{ij} = -N_{ijkl}\frac{\partial \bar{u}_k}{\partial x_l} + \Lambda_{ijk}\Omega_l$$

Convective heat flux: $$F_i^{\rm conv} = \rho c_p \langle u_i' T' \rangle = -\rho T \chi_{ij} \nabla_j \bar{s}$$

Electromotive force: $$\begin{aligned} \mathcal{E} &= \overline{\boldsymbol{u}' \times \boldsymbol{B}'} \\ &\approx \alpha \bar{\boldsymbol{B}} - \eta_{\rm T} \nabla \times \bar{\boldsymbol{B}} + \ldots \end{aligned}$$

Model vs. observed rotation

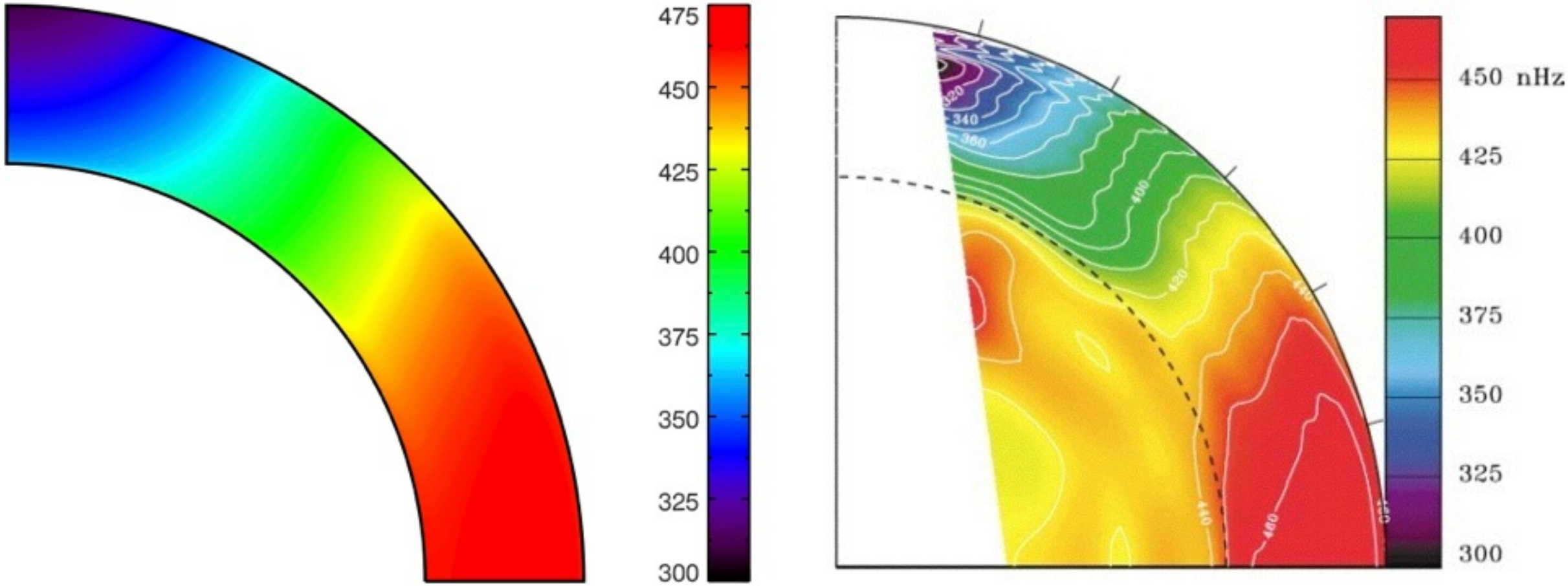

Thompson et al. 2003

Results: Sun

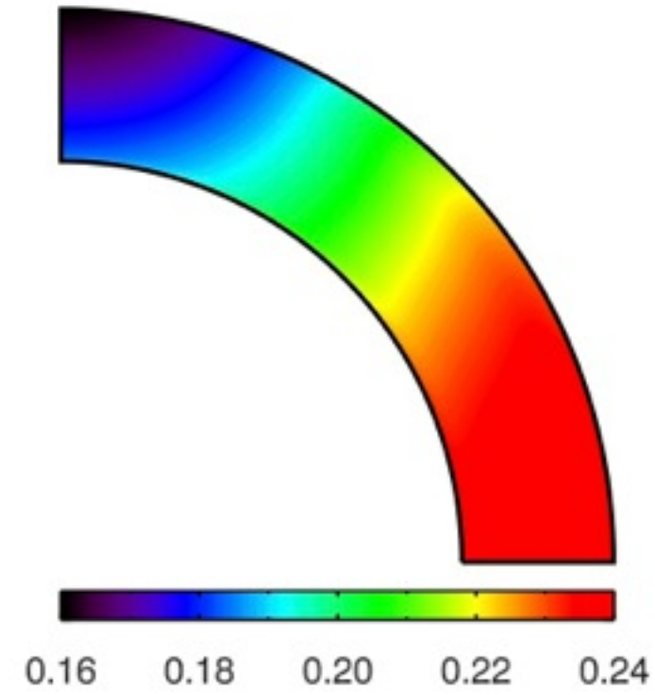
0.16
0.18
0.20
0.22
0.24

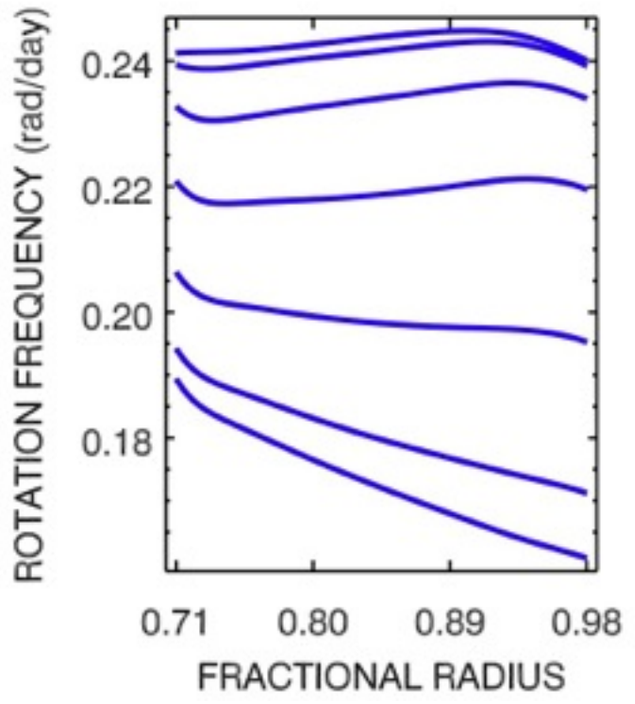
ROTATION FREQUENCY (rad/day)
0.24
0.22
0.20
0.18
0.71
0.80
0.89
0.98
FRACTIONAL RADIUS

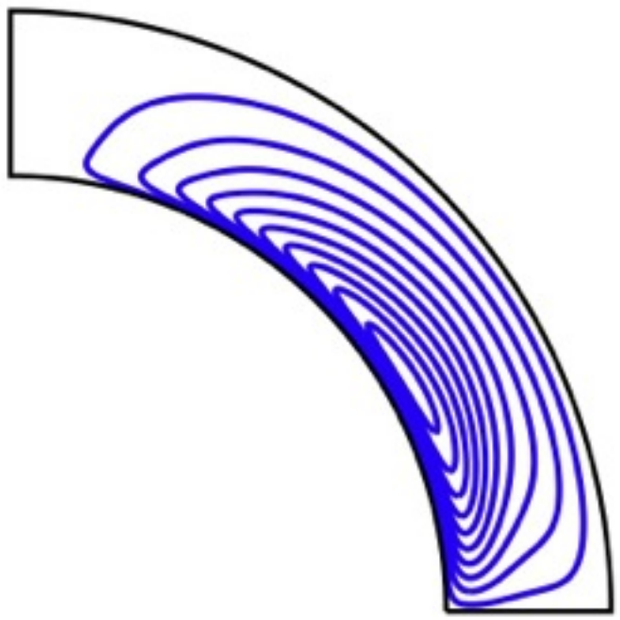

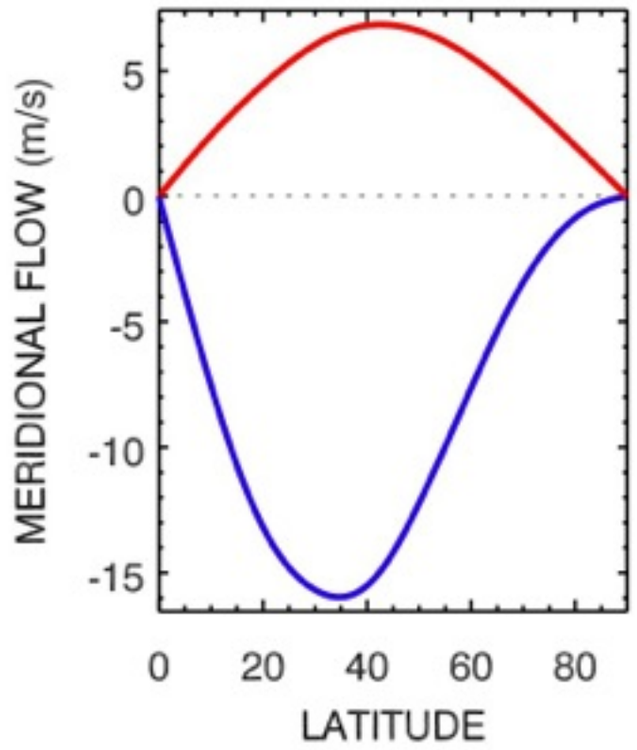
MERIDIONAL FLOW (m/s)
5
0
-5
-10
-15
0
20
40
60
80
LATITUDE

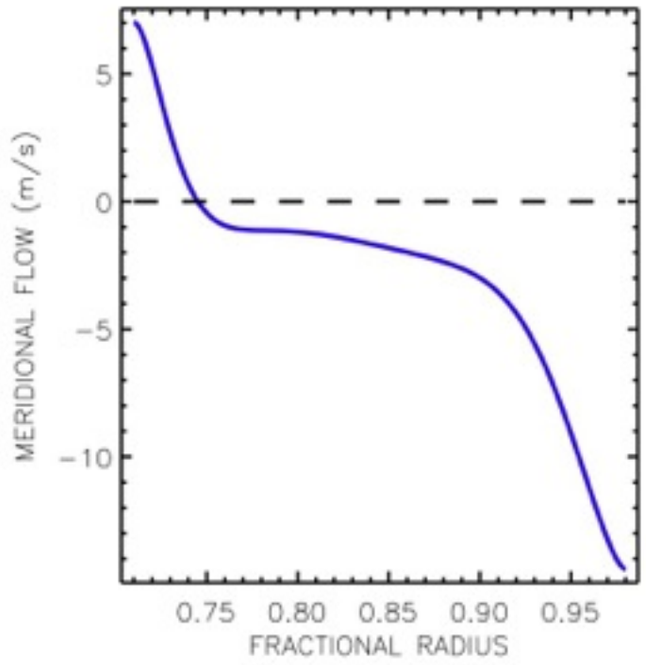
MERIDIONAL FLOW (m/s)
5
0
-5
-10
0.75
0.80
0.85
0.90
0.95
FRACTIONAL RADIUS

Thermal wind balance

Equation of motion:

$$-\left[\nabla \times \frac{1}{\rho}\nabla(\rho Q)\right]_\phi + r\sin\theta\frac{\partial\Omega^2}{\partial z} + \frac{1}{\rho^2}(\nabla\rho\times\nabla P)_\phi = 0$$

$$-\frac{1}{\rho^2}(\nabla\rho\times\nabla P)_\phi \approx \frac{g}{rc_p}\frac{\partial\bar{s}}{\partial\theta}$$

Fast rotation: $r\sin\theta\frac{\partial\Omega^2}{\partial z} - \frac{g}{rc_p}\frac{\partial\bar{s}}{\partial\theta} \approx 0$

"thermal wind balance"

not valid in boundary layers!

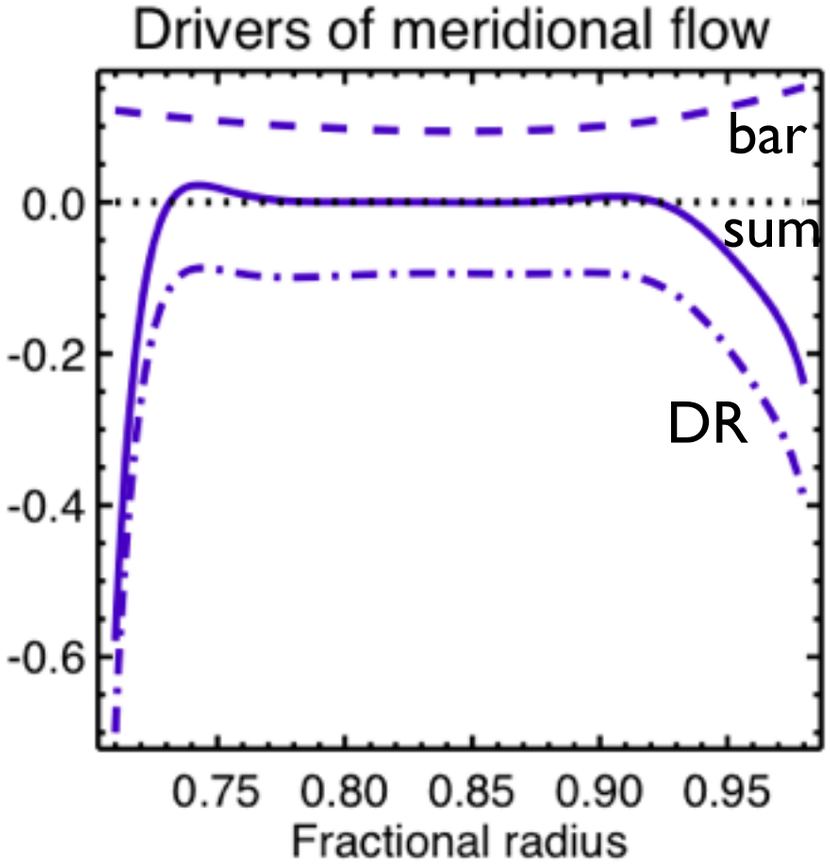

Reynolds stress vs. baroclinity

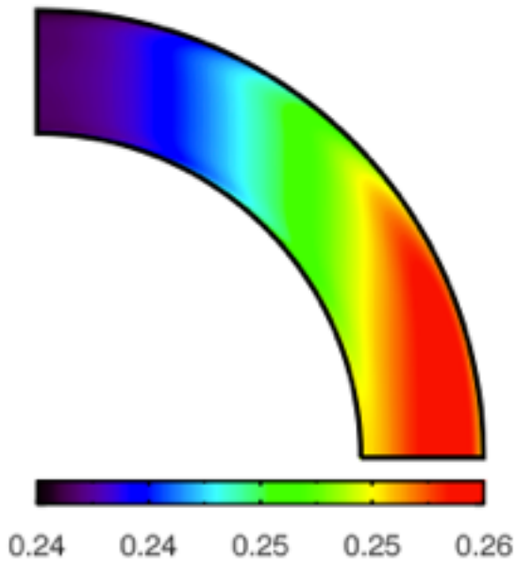

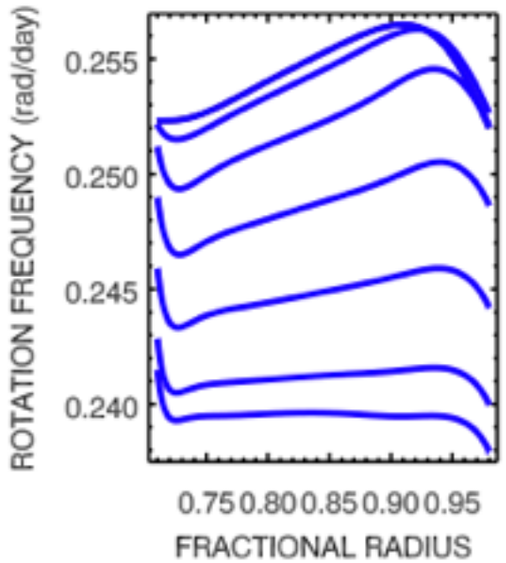

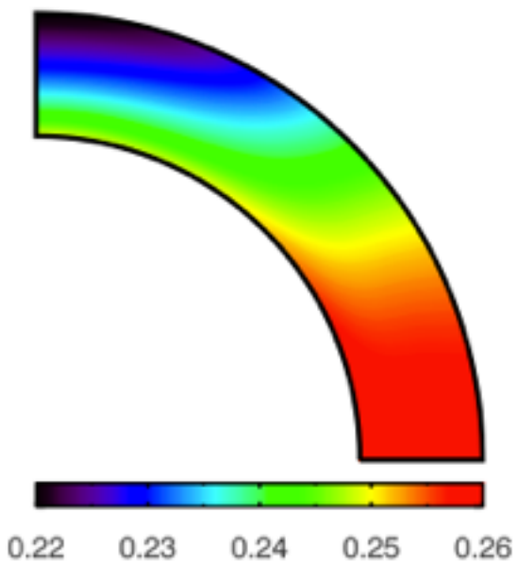

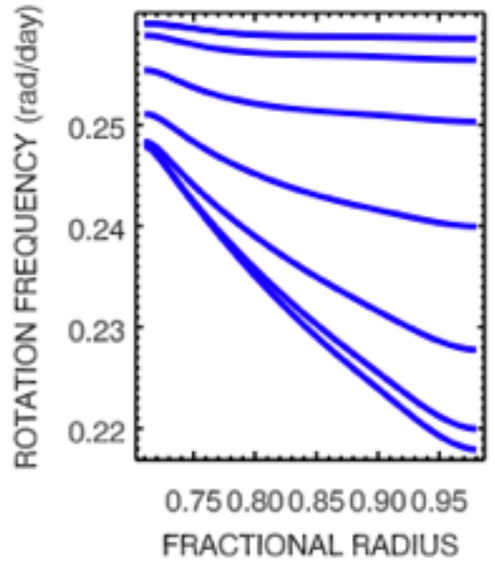

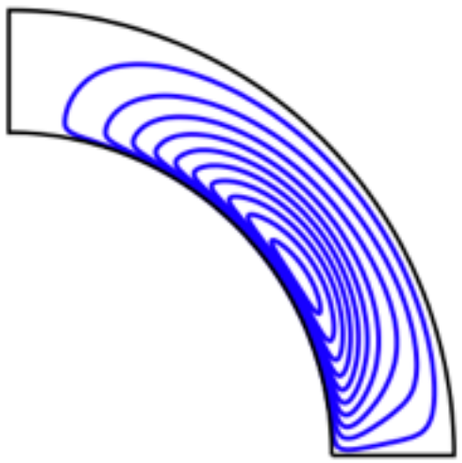

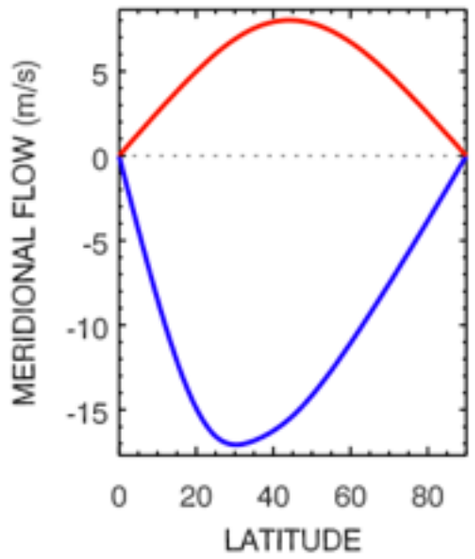

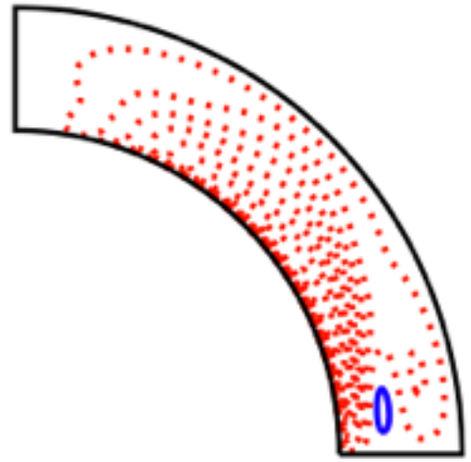

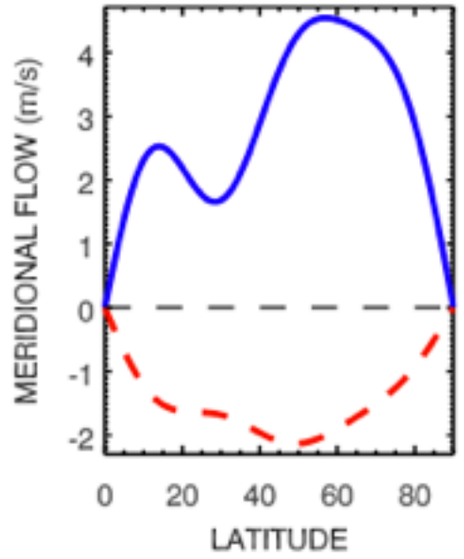

no baroclinic flow

no Λ effect

Dependence on rotation rate?

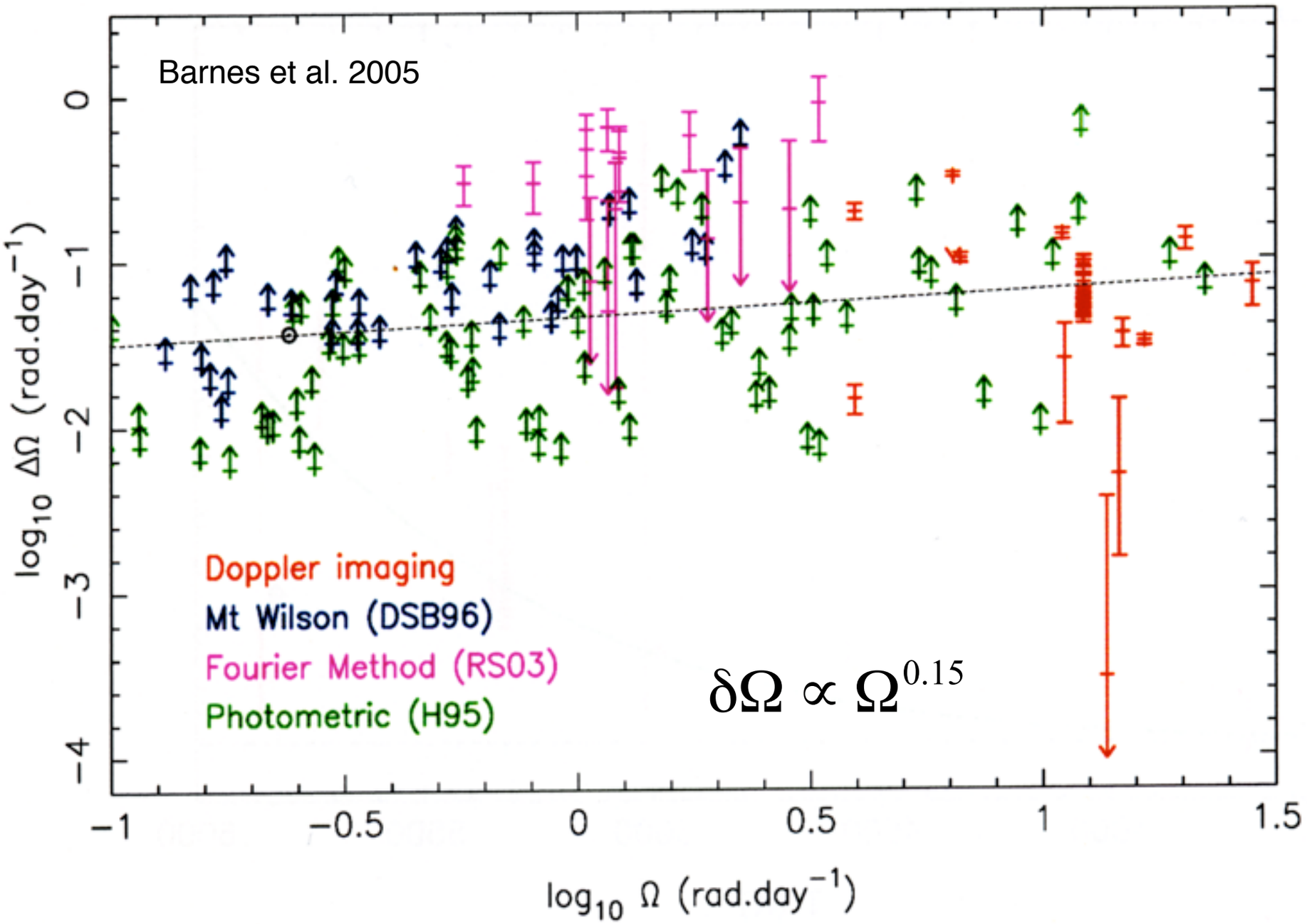

Dependence on temperature!

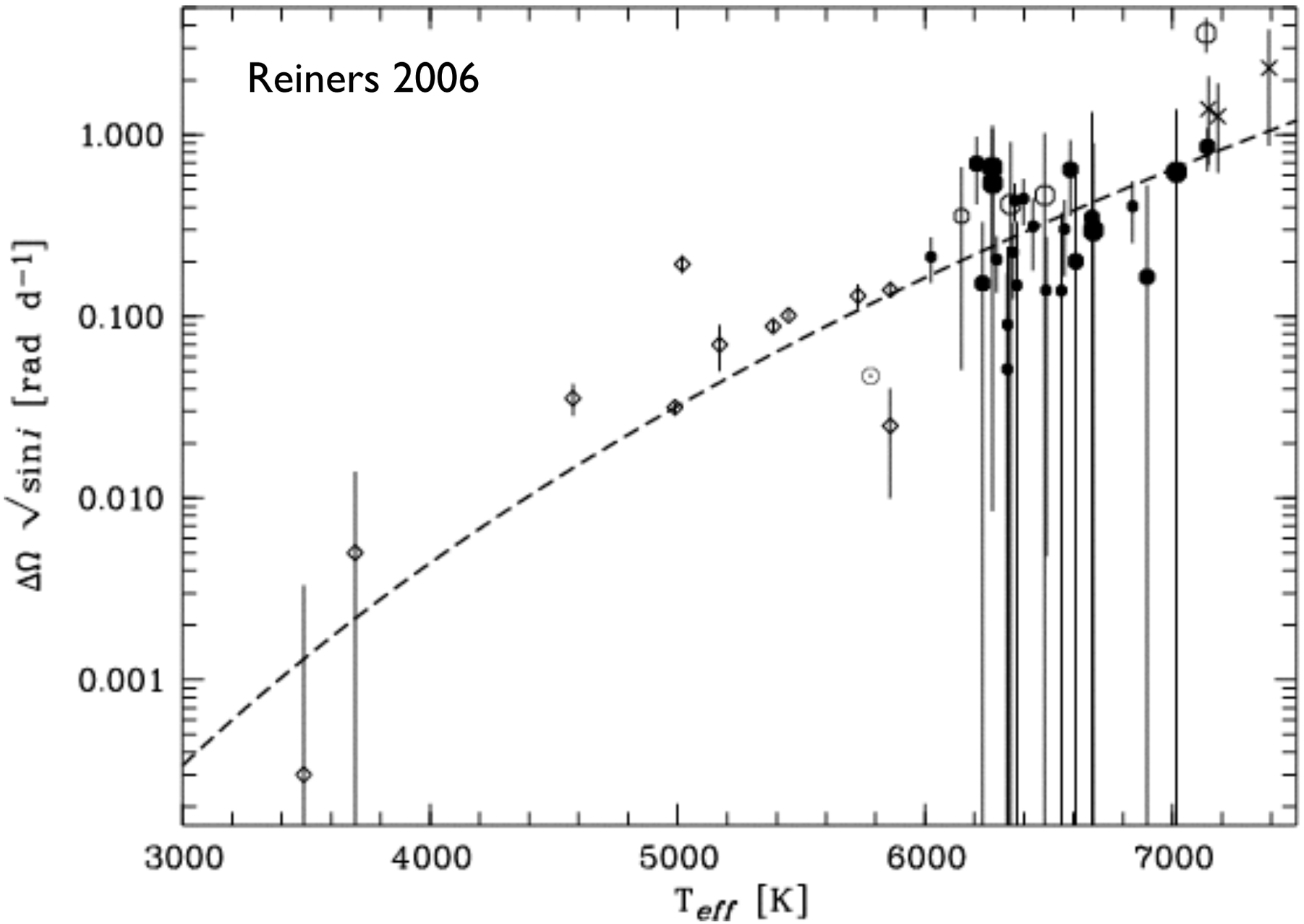

Dependence on rotation period

Differential rotation

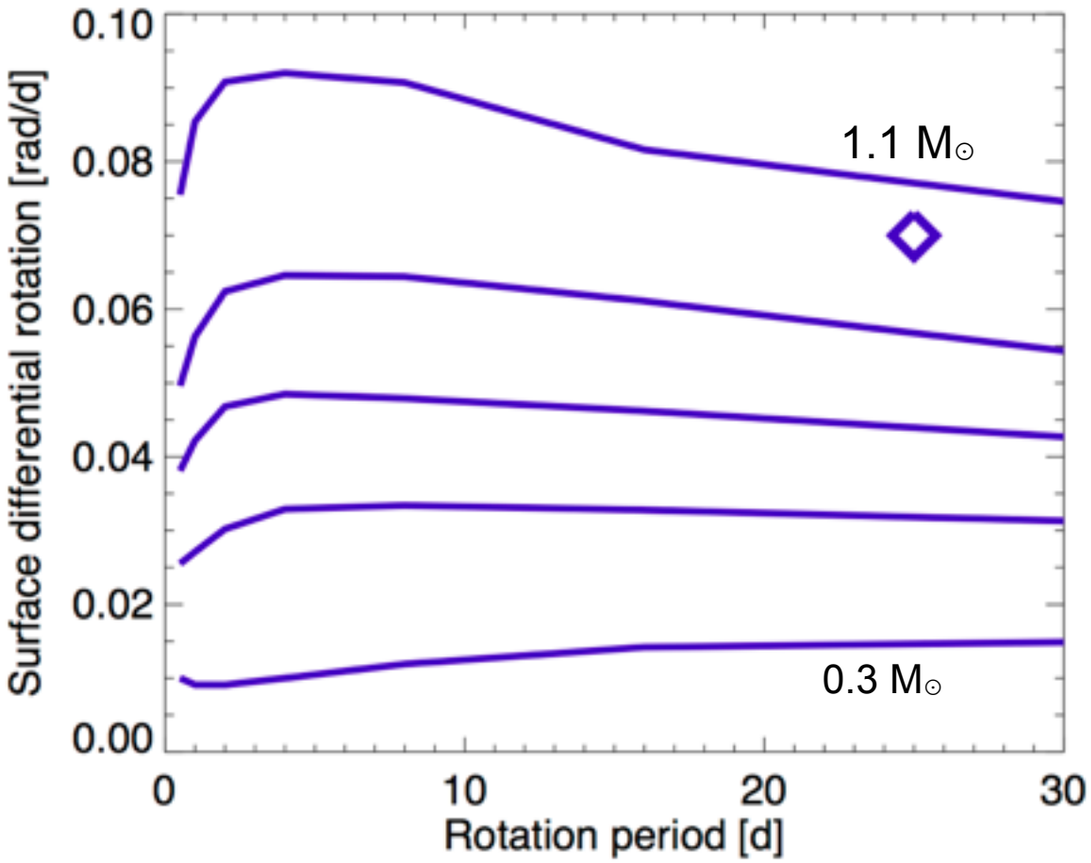

Meridional flow

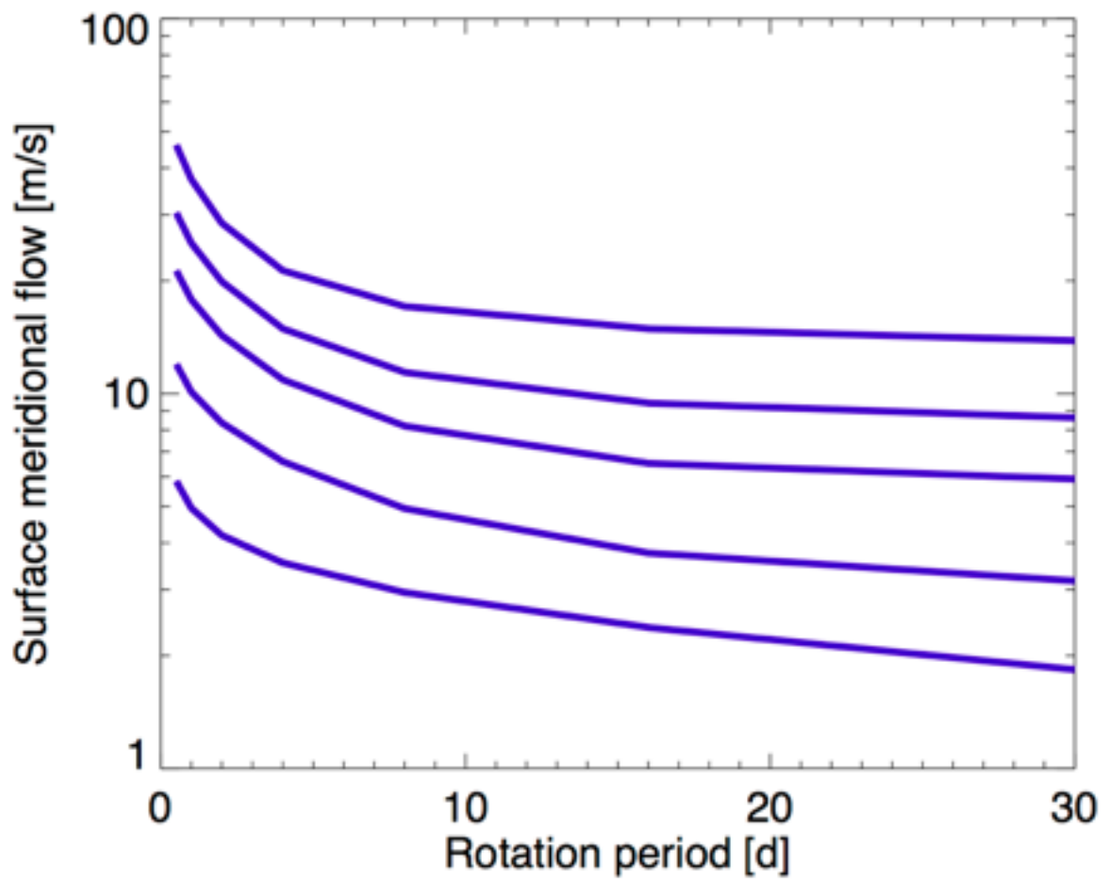

DR: model vs. observations

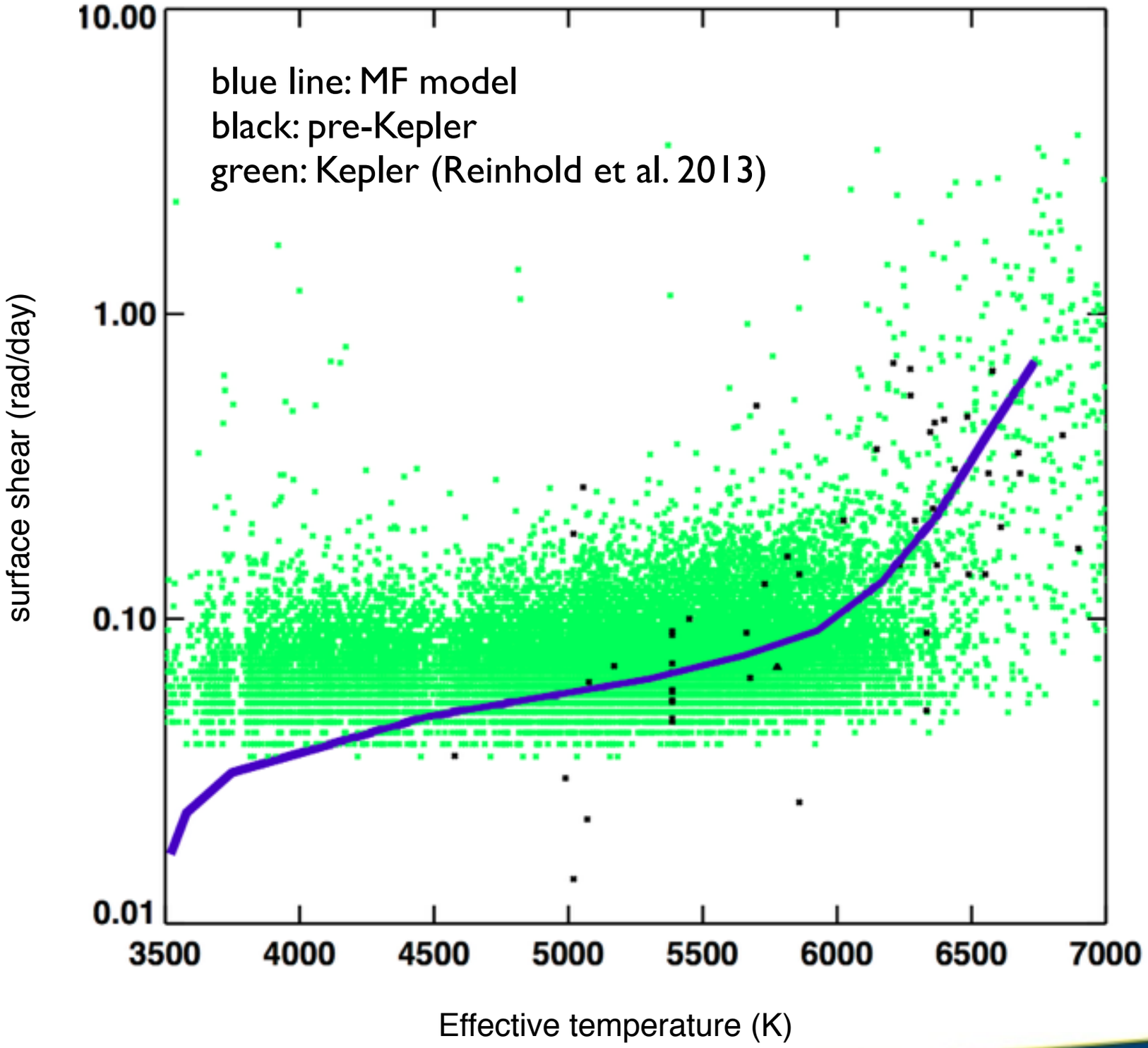

Meridional flow vs. temperature

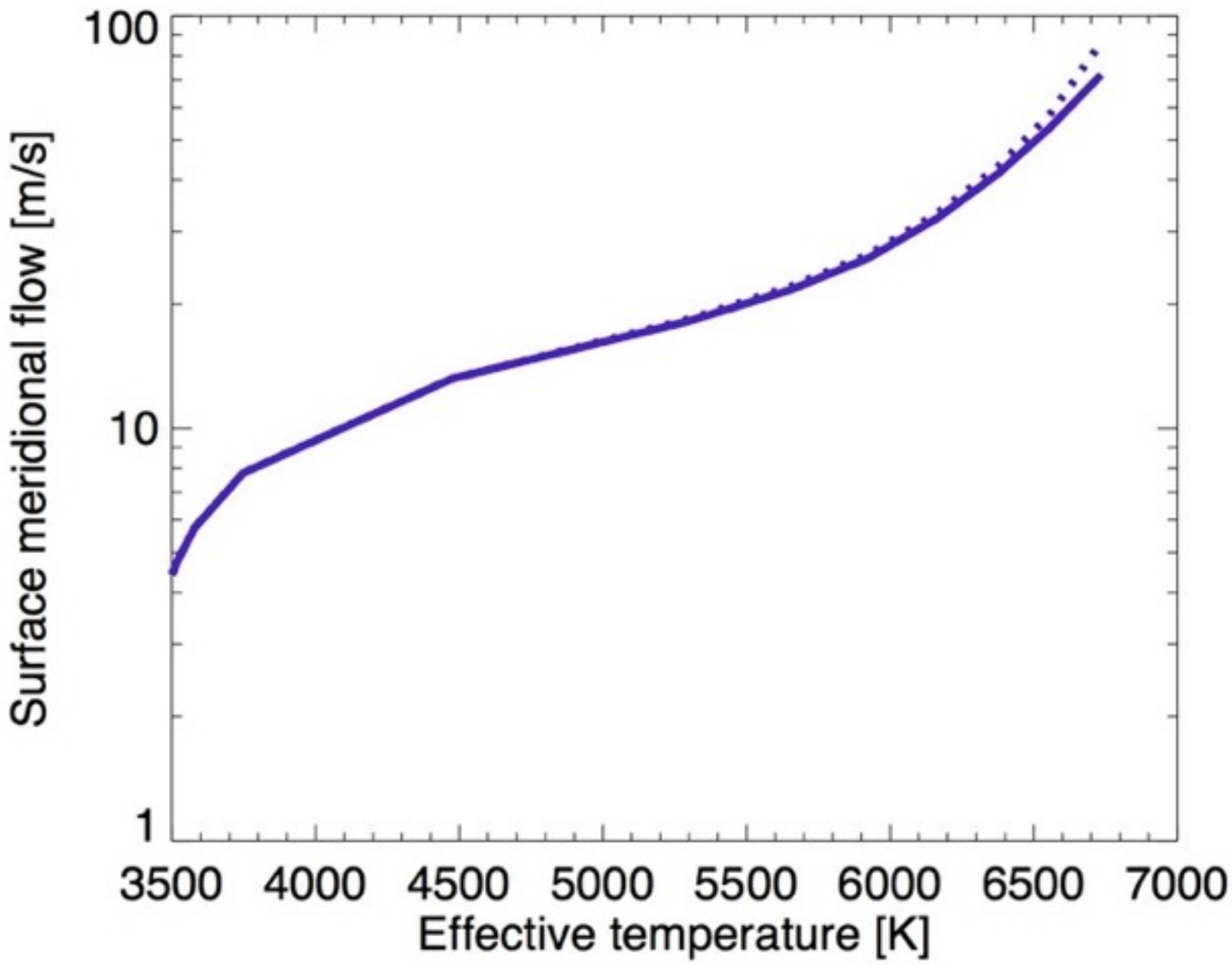

Second flow cell?

- slow rotation → second flow cell at high latitudes
- reason: disk-shaped rotation pattern

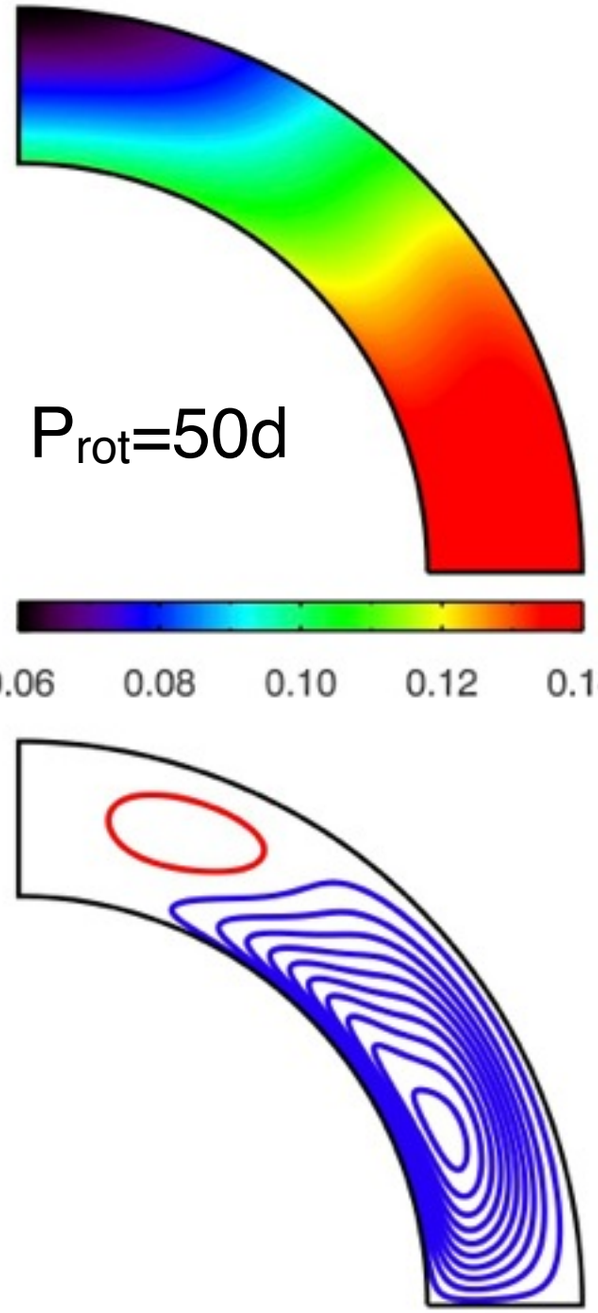

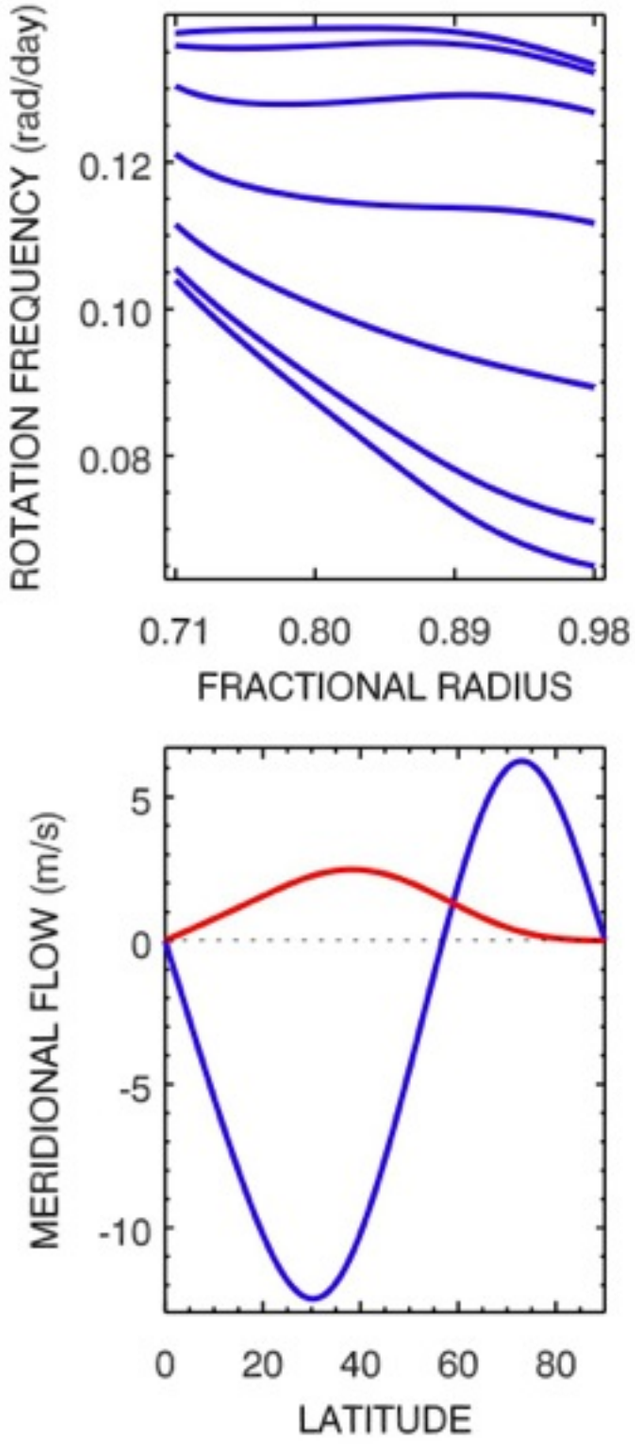

Slowly rotating Sun

P_{rot}=70d

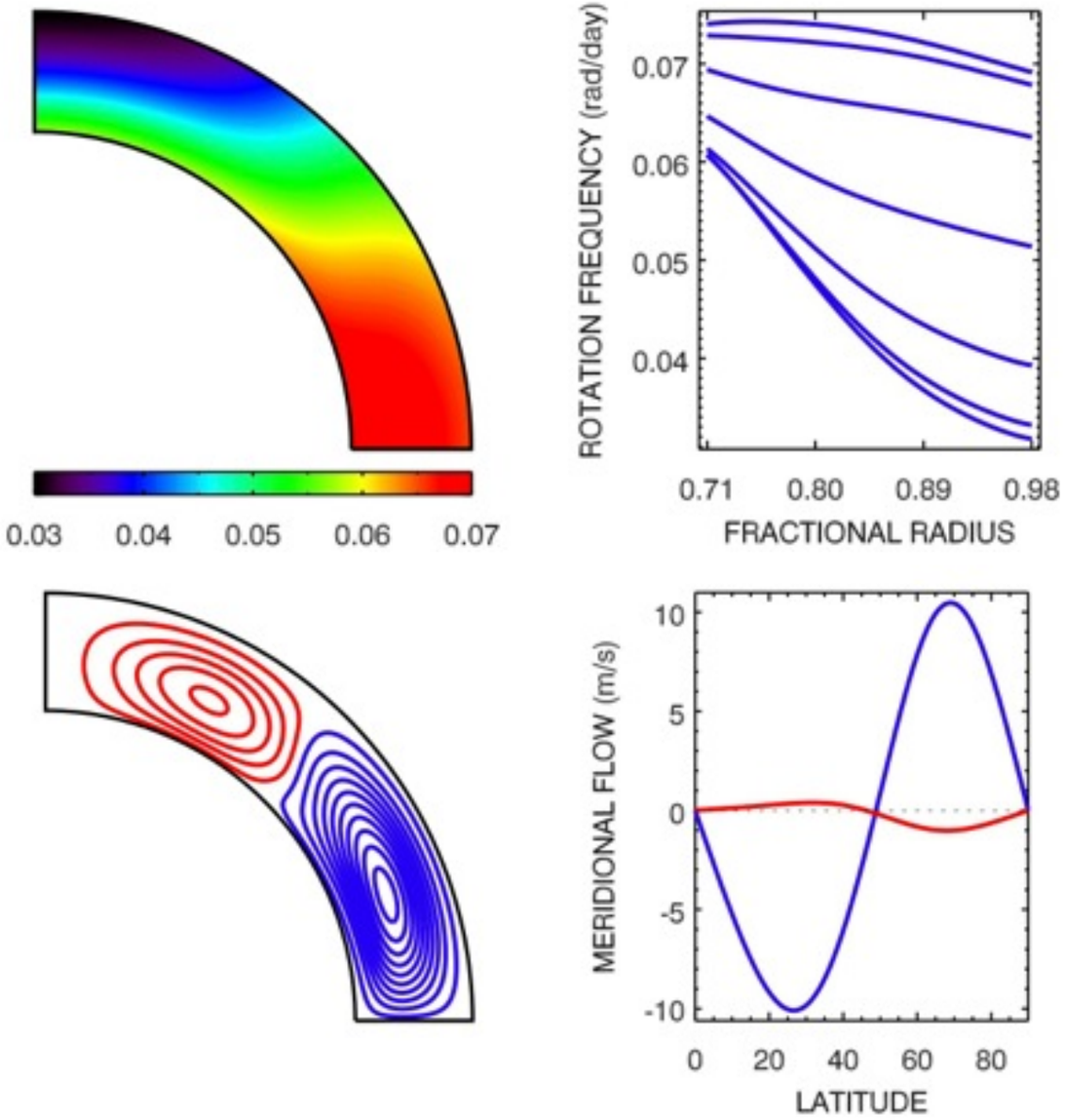

P_{rot}=140d

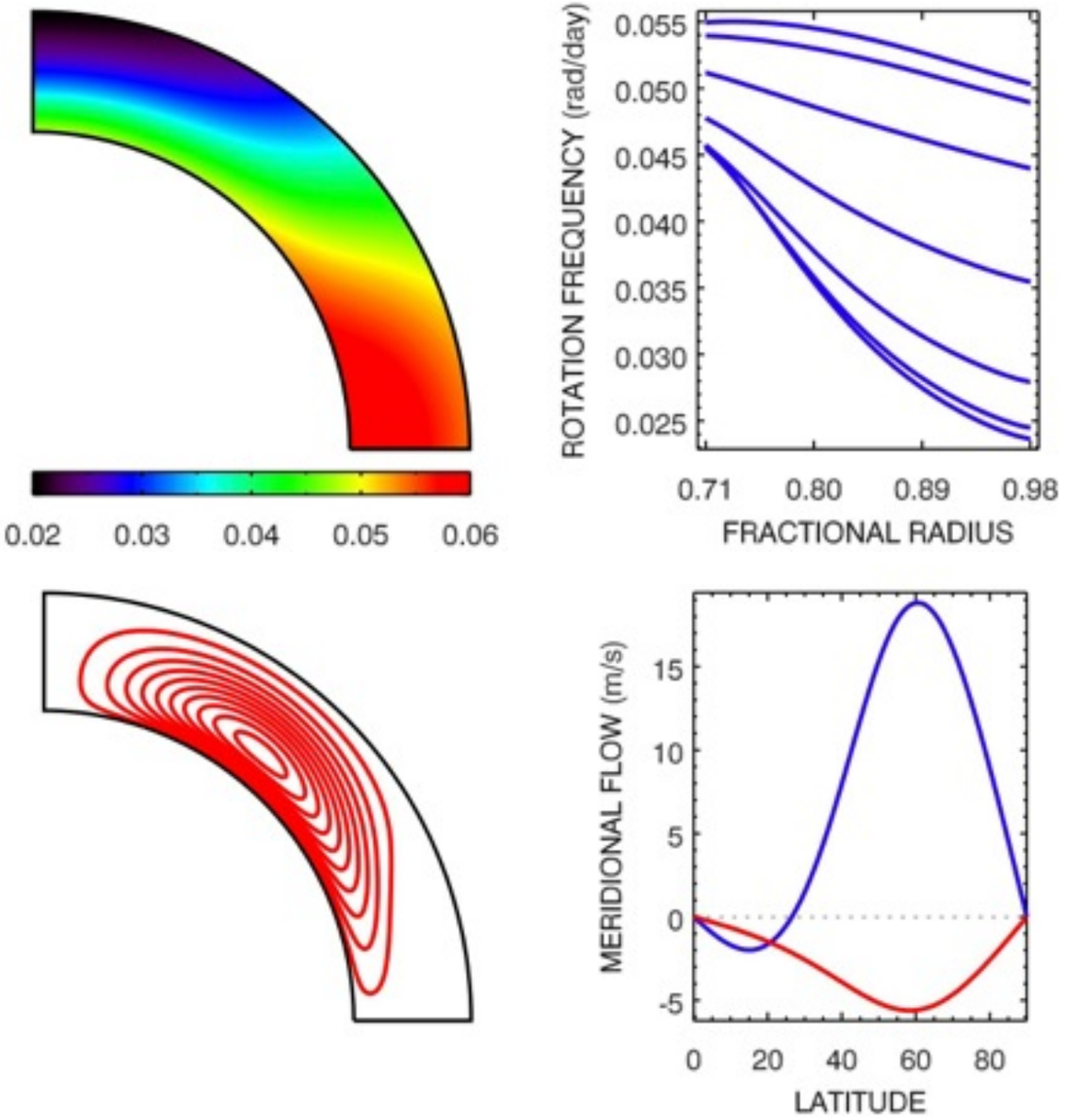

Solar tachocline

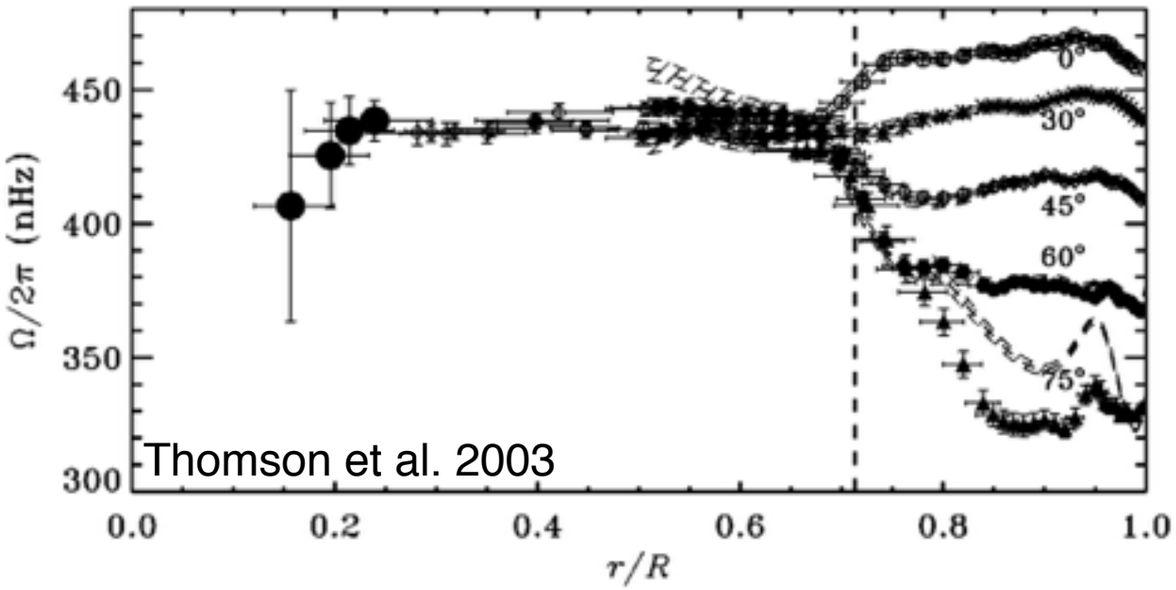

Thomson et al. 2003

- thin transition layer
- rigid rotation below CZ
- slow core rotation
- efficient transport of angular momentum into entire radiative interior
- internal magnetic field?

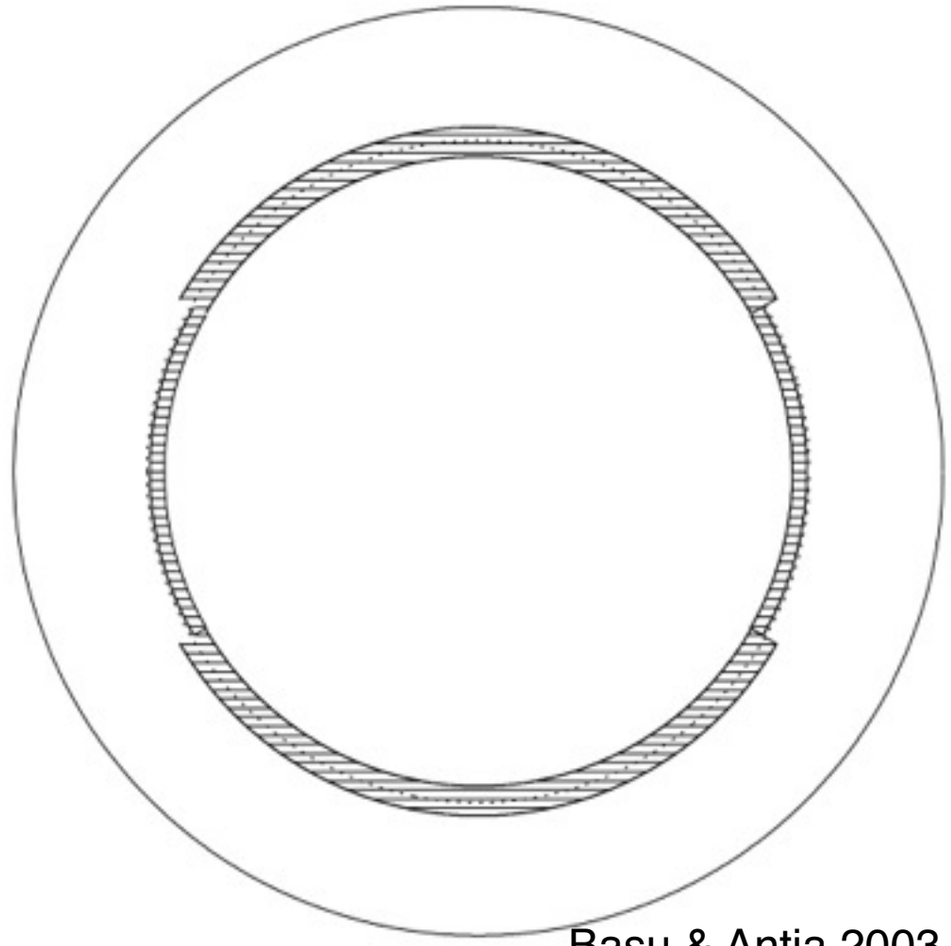

Basu & Antia 2003

FIG. 6.—Location of the tachocline inside the Sun. The shaded area is the tachocline with a half-width of $2.5w$. The dashed line shows the base of the convection zone at $r = 0.713\ R_\odot$ (Christensen-Dalsgaard, Gough, & Thompson 1991; Basu & Antia 1997).

Magnetic tachocline

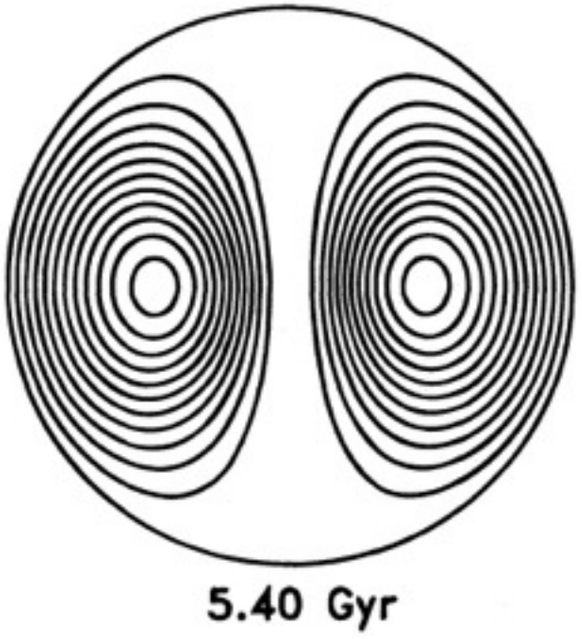

initial poloidal field

t=4.6 Gyr

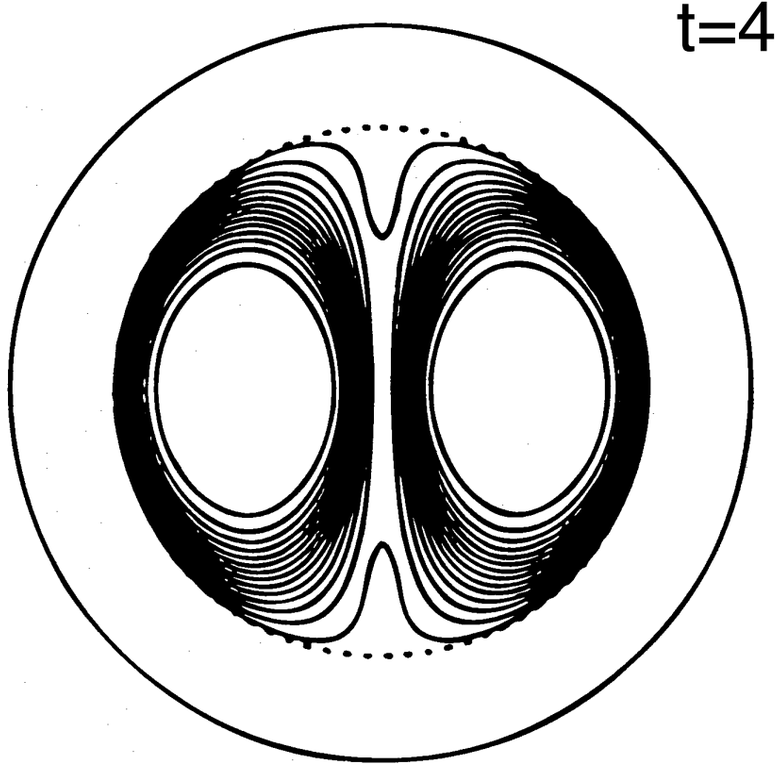

rotation rate

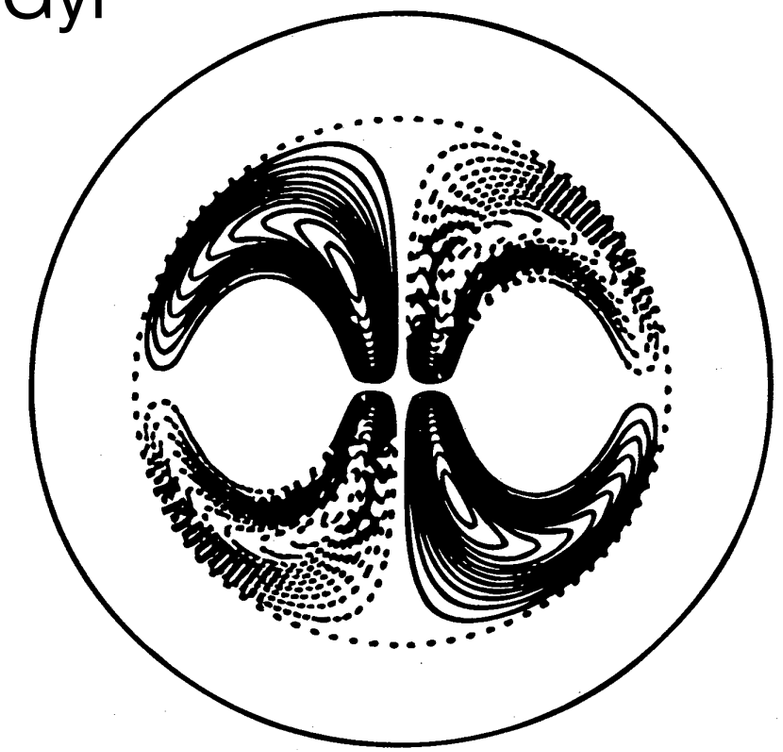

toroidal field

Rüdiger & Kitchatinov 1996

Activity-rotation relation

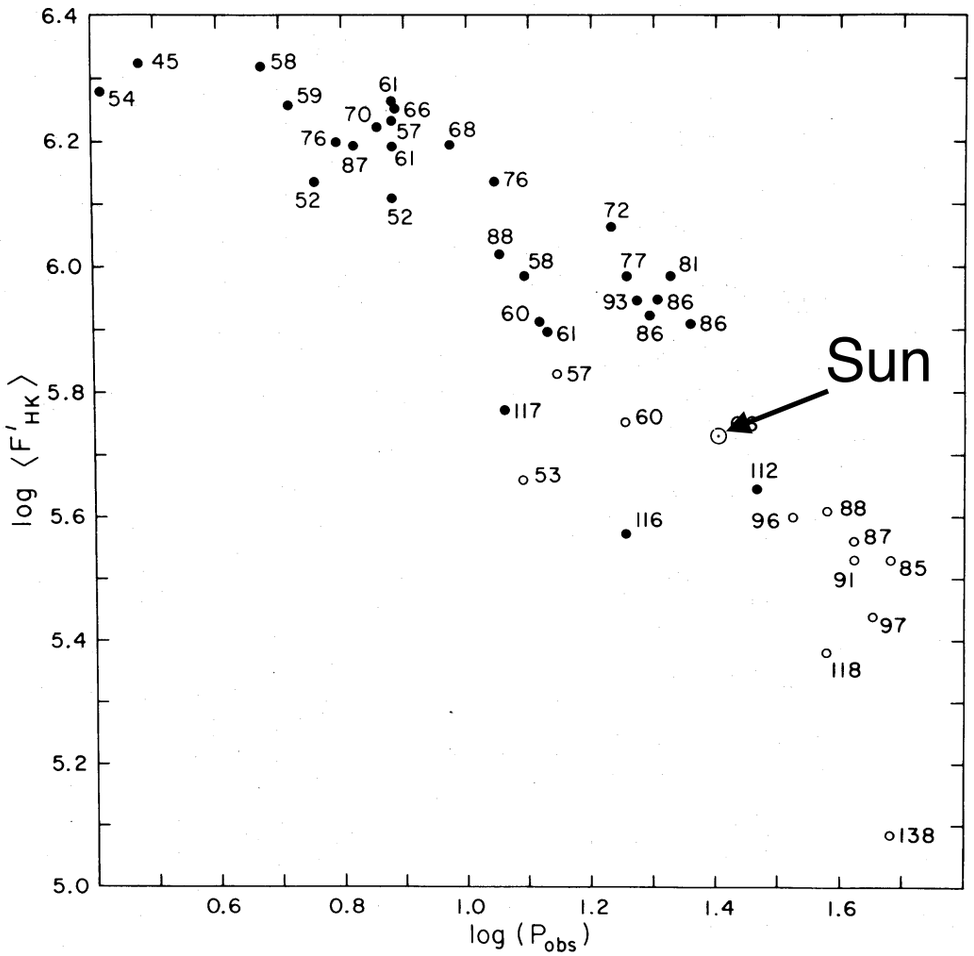

Noyes et al.1984

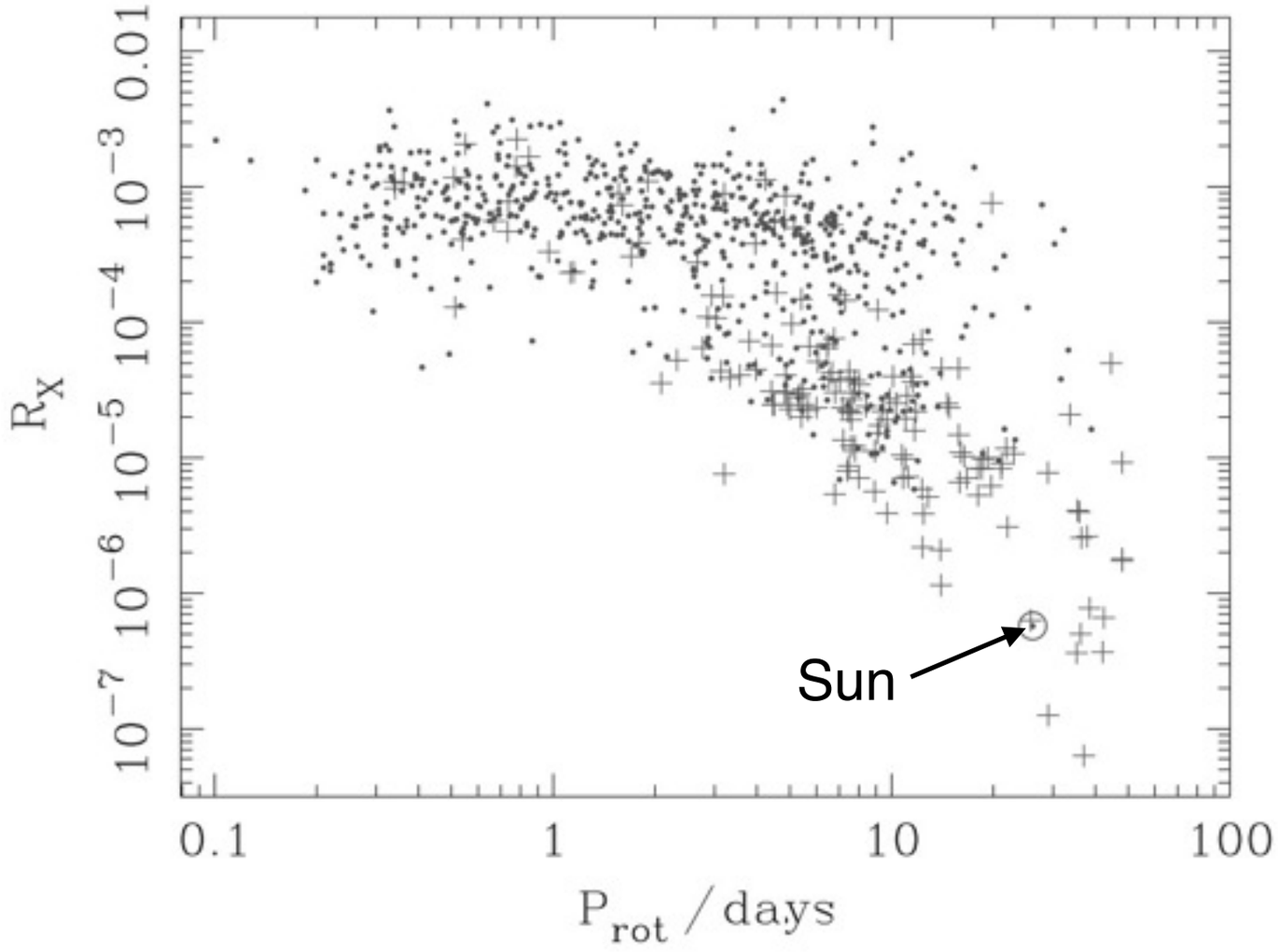

Wright et al.2011

Field strength and geometry

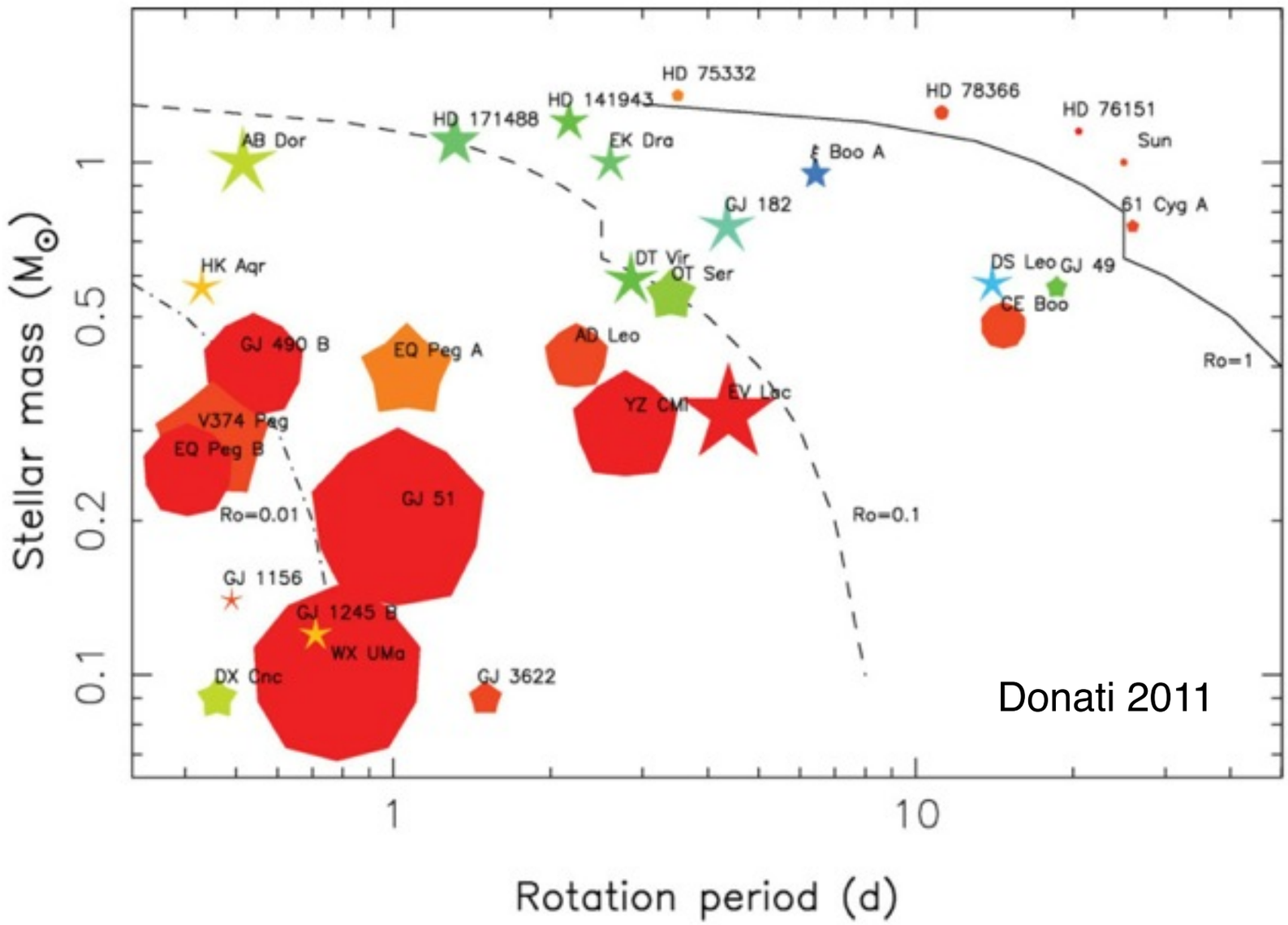

Figure 1. Basic properties of the large-scale magnetic topologies of cool stars, as a function of stellar mass and rotation rate. Symbol size indicates relative magnetic energy densities e, symbol colour illustrates field configurations (blue and red for purely toroidal and purely poloidal fields respectively) while symbol shape depicts the degree of axisymmetry of the poloidal field component (decagon and stars for purely axisymmetric and purely non-axisymmetric poloidal fields respectively). The full, dashed and dash-dot lines respectively trace where the Rossby number *Ro* equals 1, 0.1 and 0.01. The smallest and largest symbols correspond to mean large-scale field strengths of 3 G and 1.5 kG respectively (updated from Donati & Landstreet 2009).

Conclusions

- mean field model reproduces solar differential rotation and surface flow
- surface DR and meridional flow of lower MS stars
  - depend more on temperature than rotation period
  - always solar-type rotation
  - always one cell, solar-type meridional flow
- need better constraints on flux transport dynamo
- theory for tachocline and radiative zone needed
- solar stellar connection?